Journal of Metals, Materials and Minerals, 36(2), e2620, 2026

Controlled release of holy basil essential oil nanoemulsion encapsulated in gelatin/carboxymethyl cellulose hydrogel for wound care

Shehbaz AMEER[1], Pranut POTIYARAJ[1], and Tu Minh TRAN VO[1,*]

[1] *Department of Materials Science, Faculty of Science, Chulalongkorn University, Bangkok 10330, Thailand*

***Corresponding author e-mail**: minhtu.t@chula.ac.th

Received date:
29 December 2025
Revised date:
9 March 2026
Accepted date:
9 April 2026

Keywords:
Essential oil;
Hydrogel;
Gelatin;
Carboxymethyl cellulose;
Drug delivery system

Abstract

Holy basil essential oil (HBEO) is a therapeutic agent recognized for its antioxidant, anti-inflammatory, and wound-healing properties. However, its clinical use is limited by poor aqueous solubility, volatility, and instability. Nanoemulsion (NE) is an effective strategy to overcome these limitations. In this study, 1% HBEO in 0.5% polyvinyl alcohol (PVA) aqueous solution formulation yielded nanosized droplets (182±3 nm, PDI = 0.286) and showed sustained release, with 92% drug release over 30 h, compared to the rapid release for 1% HBEO in pure water. To further enhance stability and biocompatibility, the HBEO nanoemulsion (HBEONE) was incorporated into a glutaraldehyde (GA) crosslinked gelatin/carboxymethyl cellulose (CMC) hydrogel matrix. The resulting hydrogel exhibited a swelling ratio of 8 ($g \cdot g^{-1}$) and HBEO loading capacity of 67.5%. The cytotoxicity of HBEO/gelatin/CMC hydrogel was observed with less cytotoxicity compared to the natural release of HBEONE without a hydrogel matrix. These results demonstrate the HBEONE-loaded gelatin/CMC hydrogel as a robust platform for controlled release in drug delivery systems.

1. Introduction

Achieving controlled release of therapeutic agents remains a major challenge in conventional drug delivery. Traditional administration methods often cause large fluctuations in plasma drug concentrations, resulting in reduced therapeutic efficacy and an increased risk of side effects due to peak-trough variations. To address these limitations, drug delivery systems (DDSs) have been developed to transport drugs more precisely within the body, enhancing their stability, bioavailability, and therapeutic efficacy [1,2]. Among various therapeutic agents, natural bioactive agents such as essential oils (EOs) have gained significant attention due to their multifaceted pharmacological properties and biocompatibility [3]. EOs are volatile, plant-derived mixtures composed of terpenes, phenolics, and other secondary metabolites, and their incorporation into DDSs can enhance their stability, bioavailability, and targeted therapeutic action. One notable example is holy basil essential oil (HBEO), extracted from Ocimum tenuiflorum (Tulsi), a medicinal plant traditionally used widely [4]. Due to such broad pharmacological potential, HBEO is considered a promising natural therapeutic agent [5]. However, its practical use is limited due to inherent challenges like volatility, poor aqueous solubility, oxidation, and degradation [6]. Therefore, a formulation capable of protecting EOs from degradation factors is necessary. To address the drawbacks of HBEO, nanoemulsion (NE) technology offers an effective delivery strategy. These formulations are biphasic systems consisting of an aqueous continuous phase and an oil-based dispersed phase, stabilized by surfactants to ensure droplet uniformity and prevent coalescence [7]. Modern preparation techniques such as ultrasonic emulsification [8], high-pressure homogenization [9], and microfluidization [10] are commonly employed to reduce droplet size and achieve a stable nanoscale dispersion. Ultrasonic probe emulsification is considered one of the most efficient techniques for nanoemulsion fabrication. Its acoustic cavitation generates strong shear forces that produce very small, uniformly distributed droplets with enhanced interfacial stabilization and superior storage stability [11,12]. In previous studies, NE of EOs from *Cananga odorata* were prepared by ultrasonic emulsification for enhanced herbicidal potential [13]. Similarly, cinnamon and thyme essential oil nanoemulsions were prepared by the same method to improve their antifungal [14] and antibacterial [8] activities, respectively. To produce the NE, the aqueous component is typically referred to as the aqueous phase, which was designed not only as pure water but also as a diluted polymer solution, a strategy intended to reduce the volatility and evaporation of EOs components during emulsification [11]. Recent studies have demonstrated the effective use of water-soluble polymers such as polyethylene glycol (PEG) [15] and polyvinylpyrrolidone (PVP) [16] in EO-based NE systems to enhance their performance and therapeutic potential. In addition to PEG and PVP, polyvinyl alcohol (PVA) is also particularly notable for its excellent film-forming ability [17], emulsification properties, and capacity to stabilize dispersed oil droplets [18]. Thus, the present study aims to investigate the feasibility of using PVA as a continuous aqueous phase to produce NE of HBEO using an ultrasonic probe. Besides that, NE alone faces fast evaporation and short retention time on the targeted sites. Therefore, mostly NEs are incorporated into a suitable carrier that can hold the EO at the targeted site. Among these, hydrogel is the ideal carrier due to its high-water content and biocompatibility [19]. Gelatin, derived from collagen, offers excellent biocompatibility, which makes it suitable for biomedical

carriers [20]. Furthermore, carboxymethyl cellulose (CMC) is a water-soluble derivative of cellulose, which provides flexibility and enhances the swelling capacity of the hydrogel [21]. The combination of gelatin/CMC results in a stable, elastic, and highly absorbent hydrogel that is capable of long, slow, and extended release of the loaded therapeutic agents [22,23]. Earlier research has shown that CMC–gelatin composite films incorporating ε-polylysine exhibited effective antibacterial activity, maintained comparable mechanical and crystalline properties [24]. Moreover, oxidized CMC/gelatin hydrogels were reported to markedly improve wound healing outcomes in both diabetic and non-diabetic patients [25]. To increase its further structural integrity, a chemically crosslinking approach was selected using glutaraldehyde (GA), which reacts with the amino acid group of gelatin and hydroxyl groups of CMC, forming a covalent bond. For example, Bigi *et al.* reported that increasing GA concentration from 0.05% to above 1 wt% significantly enhanced the Young's modulus and reduced the swelling ratio of gelatin films, confirming that higher crosslink density leads to a more compact and mechanically resilient network [26]. However, despite the extensive use of gelatin-based scaffolds, there remains limited research on their application in hybrid gelatin/CMC hydrogels designed to encapsulate and control the release of HBEONE. Therefore, this study focuses on the development and systematic evaluation of a gelatin/CMC hydrogel loaded with HBEONE formulated in a diluted PVA solution, aiming to enhance nanoemulsion stability, achieve controlled release, and reduce cytotoxicity for biomedical applications.

2. Experimental

2.1 Materials

Gelatin with a Bloom strength of 200, pharmaceutical grade, was obtained from Spectrum Chemical Mfg. Corp. Carboxymethyl cellulose (CMC), with a degree of substitution of 0.7, was purchased from Merck Ltd., Thailand). Glutaraldehyde (GA) 25% and polyvinyl alcohol (PVA) with Mw of 115,000 Da and a hydrolysis level of 98% to 99%, were supplied by Loba Chemie Ltd. Holy Basil Essential Oil (HBEO) was sourced from TCFF Ltd., Thailand. Other reagents and chemicals were of analytical grade.

2.2 Preparation of HBEO nanoemulsion

HBEO nanoemulsions (HBEONE) were prepared following a previously reported method with slight modifications [13]. Initially, HBEO was mixed with Tween 80 in a 1:1 (w/w) ratio and magnetically stirred for 15 min to form a coarse emulsion. The coarse emulsion mixture was subjected to probe ultrasonication in the aqueous phase containing PVA solutions at varying concentrations of 0%, 0.5%, 1%, and 2% (w/w) to obtain a fine and stable nanoemulsion. Sonication was conducted using a 20 kHz ultrasonic probe at 35% amplitude for 15 min, with a pulse sequence of 30 s on and 10 seconds off. During sonication, the beaker was placed in an ice bath to dissipate the heat generated by the ultrasonic process.

2.3 Fabrication of HBEONE-entrapped gelatin/CMC hydrogels

Table 1. Different formulations of gelatin/CMC hydrogel.

Samples	Gelatin/CMC ratio	GA [% w/w]
S1	1/0	1
S2	3/1	1
S3	1/1	1
S4	0/1	1
S2-1	3/1	0
S2-2	3/1	2

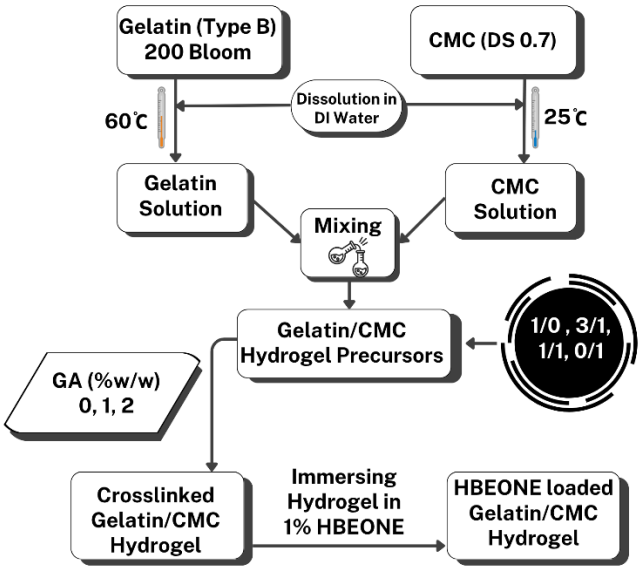

Figure 1 Schematic diagram of the fabrication of HBEONE-crosslinked gelatin/CMC hydrogels.

The hydrogels were fabricated using a previously reported method with some modifications [23], as summarized in Figure 1. A 10% (w/w) gelatin solution was prepared in deionized (DI) water at 60°C under gentle stirring. Separately, a 1% CMC solution was prepared at room temperature. Both solutions were then mixed at 50°C for 30 min under constant stirring to obtain gelatin/CMC precursor blends in different weight ratios, as shown in Table 1. Glutaraldehyde (GA) at 0%, 1.0%, and 2.0% (w/w) of the total solution was used to crosslink hydrogels, and the mixture was stirred thoroughly to ensure homogeneous dispersion. The resulting solution was cast into a Teflon mold and allowed to set at room temperature to form the hydrogel. After that, the crosslinked hydrogels were washed with DI water and 70% ethanol to remove unreacted crosslinker GA. Next, gelatin/CMC hydrogels were soaked in 1% (w/w) HBEO-NE to fully absorb. HBEONE loaded-hydrogels were rinsed with DI water 3 times, and subsequently blotted with tissue paper to remove surface water [17].

2.4 Characterization of HBEONE and gelatin/CMC hydrogels loading HBEONE

2.4.1 HBEONE droplet size and stability

The droplet size distribution and polydispersity index (PDI) of the HBEONE were determined using a dynamic light scattering (DLS) instrument (Zetasizer, Malvern Panalytical, UK) to evaluate stability as well as uniformity of HBEONE. Samples were diluted with DI

water in a 1:9 ratio to avoid the multiple scattering effect. 2 mL diluted sample was transferred into a cuvette for analysis. Measurements were conducted at 25°C and a fixed scattering angle of 165°. Each sample was analyzed in triplicate, and the average droplet size and PDI were recorded.

The stability of the HBEONE was assessed by centrifuging 10 mL samples at 10,000 rpm for 20 min (25°C). Stability was evaluated for 8 weeks at 4°C and 25°C, representing refrigerated and ambient storage conditions, respectively. These conditions were selected to simulate standard pharmaceutical shelf-life and evaluate the retention of volatile HBEO components under varying thermal stresses [27,28].

2.4.2 Characterization of gelatin/CMC composite hydrogels

Chemical structure confirmation

Attenuated Total Reflectance–Fourier Transform Infrared (ATR-FTIR) spectroscopy was performed to identify the functional groups and the interactions of gelatin, CMC, HBEONE, and HBEONE-loaded gelatin/CMC hydrogels. 32 scans per sample over the spectral range of 4000 cm^{-1} to 400 cm^{-1} were recorded with a resolution of 2 cm^{-1}.

Rheological measurement

Rheological analysis was conducted to check the viscoelastic behavior of gelatin/CMC hydrogels. Rheometer (HAAKE MARS 40) equipped with a P20-CTC/Ti rotor geometry was used for measurements. Amplitude sweep tests were performed at 1 Hz with a strain range of 0.1% to 500% to determine the linear viscoelastic region (LVR) for each gelatin/CMC composite hydrogel. Storage modulus (G′) and loss modulus (G″) were recorded.

Thermal stability of hydrogels

Differential Scanning Calorimetry (DSC) was performed to check the stability, thermal transition, and the effect of the incorporation of HBEONE in gelatin/CMC hydrogel systems. The analysis was conducted over a temperature range of 25°C to 210°C at a heating rate of 10°C·min^{-1} under a nitrogen atmosphere.

Morphology observation

The cross-sectional morphology of pure gelatin, gelatin/CMC composite, and HBEONE-loaded CMC/gelatin hydrogel was investigated using scanning electron microscopy (SEM, JEOL JEM-6335F). Before imaging, samples were lyophilized and coated with a thin layer of gold using a sputter coater to increase conductivity. SEM images were captured to evaluate the interconnectivity within the hydrogel matrix.

Swelling degree

The swelling behavior of gelatin, CMC, and combined gelatin/CMC hydrogels was evaluated to check the water absorption capacity. The swelling tests were conducted in phosphate-buffered saline (PBS) at 37°C to simulate the physiological conditions [29]. The hydrogels were immersed in PBS until equilibrium, and the swelling degree was calculated using the following equation:

$$\text{Swelling degree} = \frac{W_s - W_d}{W_d} \quad (1)$$

where W_s is the weight of the swollen material, and W_d is the weight of the dry material.

2.4.3 HBEONE entrapment efficiency and in vitro release study

HBEO entrapment efficiency was evaluated by the previously reported method with modifications [30]. Gelatin/CMC hydrogel and HBEONE-loaded gelatin/CMC hydrogel were cut into pieces of 0.6 cm × 3 cm and sandwiched using quartz plates and placed into a UV-Vis. In Figure 2, the presence of HBEO was confirmed by measuring the intensity of its characteristic absorption peak at 278 nm in the UV-Vis spectrum. The absorption spectrum of the HBEO-NE-loaded hydrogel exhibited a prominent peak at 278 nm, indicating the successful incorporation of HBEO within the hydrogel matrix.

The release behavior of HBEO from the HBEONE-loaded gelatin/CMC hydrogels was conducted in 100 mL of PBS (pH 7.4) maintained at 37.0±1°C to mimic body temperature.

At intervals, 3 mL samples were withdrawn and replaced with fresh PBS to maintain constant volume. The amount of HBEO released was quantified by UV-Vis spectrophotometry at 278 nm. All release experiments were performed in triplicate (n = 3), and results are reported as mean ± standard deviation. The initial 60% release data were fitted to the following kinetic models to elucidate the mechanism of HBEO release from the hydrogel matrix [31]:

Korsmeyer–Peppas model

$$\left(\frac{M_t}{M_\infty}\right) = \text{Ktn} \quad (3)$$

Where M_t is the amount of HBEO released at time t, M_∞ is the total release at equilibrium, K is the release rate constant, and n is the release exponent (Fickian if $n \leq 0.45$, non-Fickian if $0.45 < n < 1$).

Zero-order model

$$C_t/C_0 = k_0 t \quad (4)$$

First-order model

$$\log C_t = \log C_0 - \frac{k_1 t}{2.303} \quad (5)$$

Higuchi model

$$C_t/C_0 = k_h t^{0.5} \quad (6)$$

where C_t represents the amount of drug released at time t, C_0 denotes the initial drug concentration within the hydrogel, k_0, k_1, and k_h correspond to the respective release rate constants, and n is the release exponent that characterizes the mechanism of drug release.

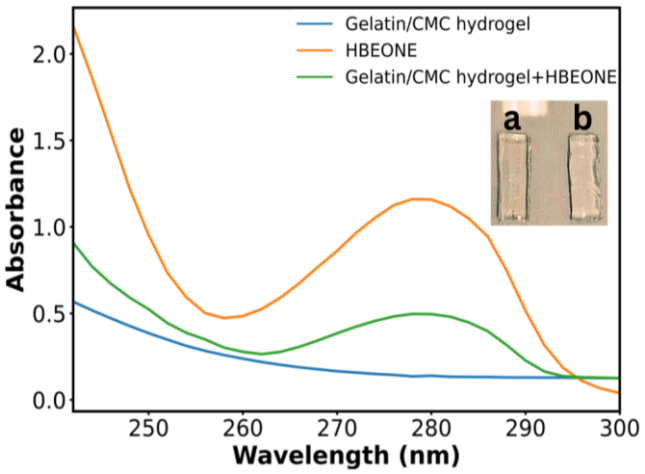

Figure 2. UV–vis spectra of the gelatin/CMC hydrogel and gelatin/CMC/HBEO-NE hydrogel with 2.1 mm and 1.95 mm thickness, respectively, and HBEONE at 166.7 ppm; the appearance of gelatin/CMC hydrogels (a) without HBEONE, and (b) with HBEONE (the insert picture).

Antioxidant test

The antioxidant potential of HBEO-NE-loaded gelatin/CMC hydrogel was evaluated using the DPPH (2,2-diphenyl-1-picrylhydrazyl) radical scavenging assay [29]. A 0.1 mM DPPH solution was prepared in ethanol. HBEONE-loaded hydrogel was immersed in the PBS solution at pH 7, and 3 mL sample was taken out after intervals. Each sample was mixed with DPPH solution and incubated in the dark for 30 min. Absorbance was measured at 517 nm using a UV-Vis spectrophotometer. Ethanol served as the blank condition, and the DPPH solution was used as the control. The DPPH radical scavenging activity was calculated using the following equation:

$$\text{Scavenging activity (\%)} = \left(\frac{A_{Control} - A_{Sample}}{A_{Control}}\right) \times 100 \qquad (2)$$

where $A_{Control}$ is the absorbance of the DPPH solution without the sample, and A_{Sample} is the absorbance after the sample was added. The antioxidant activities of the HBEONE-loaded and blank hydrogels were compared to check the retention of bioactivity of HBEO after encapsulation.

Cytotoxicity evaluation using MTT Assay

The cytotoxicity of HBEONE and HBEONE-loaded gelatin/CMC hydrogel was checked using MTT (3-(4,5-dimethylthiazol-2-yl)-2,5-diphenyltetrazolium bromide) assay [32]. 100 µL of L929 fibroblast cell suspension solution was seeded into 96-well plates at a density of $5 \times 10_4$ cells·mL^{-1} and incubated at 3°C in a humidified atmosphere containing 5% CO_2 for 24 h to allow cell attachment. After incubation, the DMEM (Dulbecco's Modified Eagle Medium) culture medium was replaced with fresh medium containing the prepared hydrogel extracts, and cells were further incubated for 48 h. Subsequently, MTT solution (0.5 mg·mL^{-1}) was added to each well, and the plates were incubated for an additional 4 h to allow the formation of formazan crystals. The supernatant was then carefully removed, and 100 µL of DMSO was added to each well to dissolve the formazan crystals completely. The absorbance was measured at 570 nm using a Microplate Reader, Ensight™, Multimode, Perkin Elmer, and cell viability (%) was calculated using the following equation:

$$\text{Cell viability} = \left(\frac{A_{Sample}}{A_{Control}}\right) \times 100\ (\%) \qquad (7)$$

Where $A_{Control}$ is the absorbance of the untreated conditions without samples. A_{Sample} is the absorbance of the treated sample.

A one-way analysis of variance (ANOVA) with Tukey's test was used to determine the statistical significance among groups. The level of significance was set at $p^* < 0.05$, and all analyses were conducted using SPSS version 30.0.0 software. All data are presented as the mean ± standard deviation (SD) of three independent replicates.

3. Results and discussion

3.1 Impact of emulsification conditions on NE characteristics

As shown in Table 2 and Figure 3, the droplet size and stability of HBEONE were significantly affected by the PVA content in the aqueous phase. The nanoemulsion formulated in DI water exhibited the smallest droplet size (124 nm) with a moderate PDI (0.269), showed a lower equilibrium HBEO release (85%), likely due to the absence of a polymer (PVA), which caused partial volatilization of HBEO. Upon incorporation of PVA at 0.5% PVA, the droplet size increased slightly to 182 nm (PDI 0.286). The greatest equilibrium release of HBEO at 0.5% PVA was attributed to an optimal balance between interfacial stabilization and diffusion surface area. Although the formulation without PVA produced a smaller NE droplet size, the absence of PVA led to poor volatile retention and premature loss. Furthermore, increasing PVA concentration (1% to 2%) increased droplet size and PDI. The higher aqueous-phase viscosity and large droplet size reduced the diffusion rates and consequently lowered HBEO release. Visual stability studies showed that 0.5% to 1% PVA formulations maintained better stability after 8 weeks at 4°C. At 25°C, Ostwald ripening caused the more pronounced phase separation and creaming in all formulations.

Table 2. Effect of PVA concentrations on the size, stability, and release of HBEO from HBEONE.

Oil phase	Aqueous phase (PVA solution)	Droplet size [nm]	Polydispersity index (PDI)	Release of HBEO at Equilibrium [%]
1%	0%	124±3	0.269±0.05	85±3
	0.5%	182±3	0.286±0.05	92±3
	1%	244±3	0.242±0.05	88±3
	2%	394±3	0.302±0.05	85±3

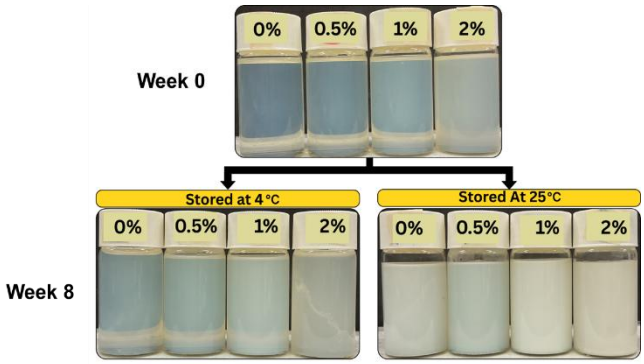

Figure 3 Stability comparison of HBEO-NE in 0 % to 2 % PVA solution at 4°C and 25°C after 8 weeks.

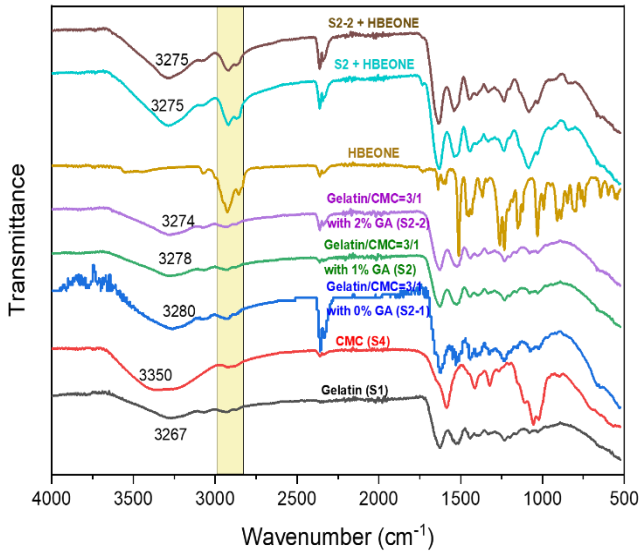

Figure 4. FTIR spectra of gelatin/CMC hydrogels showing the effect of the incorporation of HBEO.

3.2 Characterization of HBEONE entrapped gelatin/CMC hydrogels

3.2.1 Chemical structure confirmation of the composite hydrogels

FTIR analysis was performed to investigate the interactions between gelatin, CMC, and the crosslinked gelatin/CMC hydrogel, both with and without the incorporation of HBEONE (Figure 4). The spectrum of neat gelatin displays an absorption band at around 3267 cm^{-1}, corresponding to the stretching vibration of –OH and –NH groups involved in hydrogen bonding.

The amide I band appears at 1629 cm^{-1}, attributed to C=O stretching vibration, confirming the characteristic protein backbone. In the spectrum of pure CMC, a strong –OH stretching band is observed at 3350 cm^{-1}. When gelatin and CMC were blended (S2-1), the –OH/–NH stretching peak was at 3280 cm^{-1}, and it was slightly shifted to a lower wavenumber, indicating the formation of hydrogen bonding between the hydroxyl groups of CMC and the amide groups of gelatin by increasing the crosslinker GA to 2%. As highlighted in the yellow-shaded region, the significant absorption features appeared around 2952 cm^{-1}, which are attributed to the C–H stretching of aliphatic constituents of HBEO, emphasizing the successful incorporation of HBEONE into the hydrogel matrix.

However, these peaks exhibited a slight reduction in intensity at 2% GA compared to 1% GA, suggesting a lower HBEONE entrapment due to the denser and more compact crosslinked network.

3.2.2 Rheological properties of composite hydrogels

The viscoelastic behaviour of composite hydrogels was shown in Figure 5. G' value of neat gelatin (S1) was slightly enhanced to 8200 Pa by incorporating CMC into the hydrogel matrix at the ratio of 3:1 (S2) and dropped to 4000 Pa when gelatin: CMC was 1:1 due to an increase in the overall hydrophilicity and water uptake of the matrix. Moreover, G' value was significantly improved at higher GA content at 2% and the gel structure became less elastic than that 1% GA because of greater crosslink density at higher crosslinker concentration. Additionally, the entrappment of HBEONE into the hydrogel matrix resulted in the softening of the hydrogel. Interestingly, these composite hydrogels exhibited outstanding elastic performance, maintaining structural integrity and a predominantly elastic response at strains exceeding 200% before network collapse, highlighting their strong potential for biomedical applications, particularly as flexible and mechanically resilient wound-dressing materials.

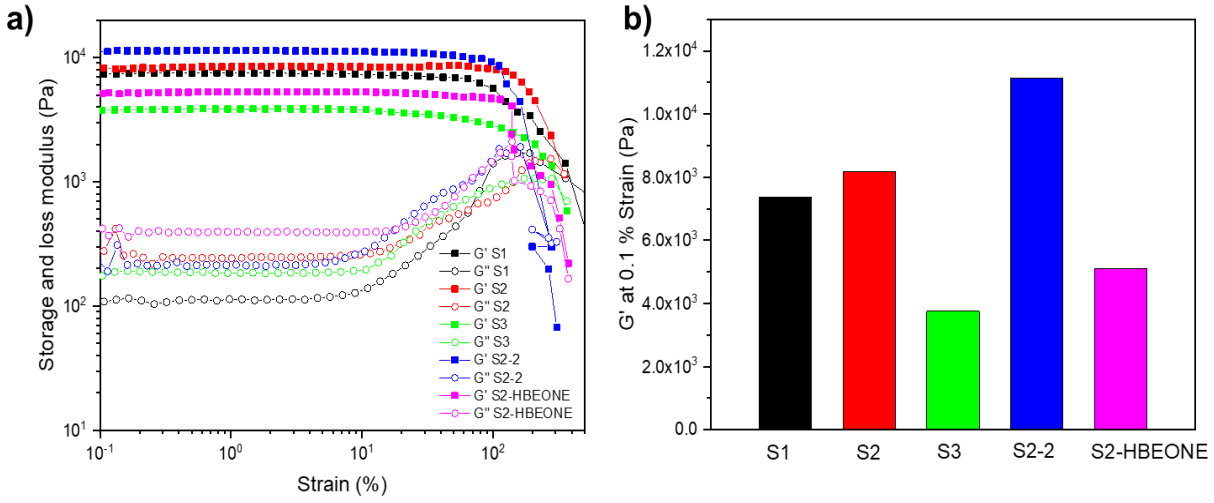

Figure 5. (a) Storage (G') and loss (G") modulus of hydrogels, and (b) the G' value at 0.1% strain.

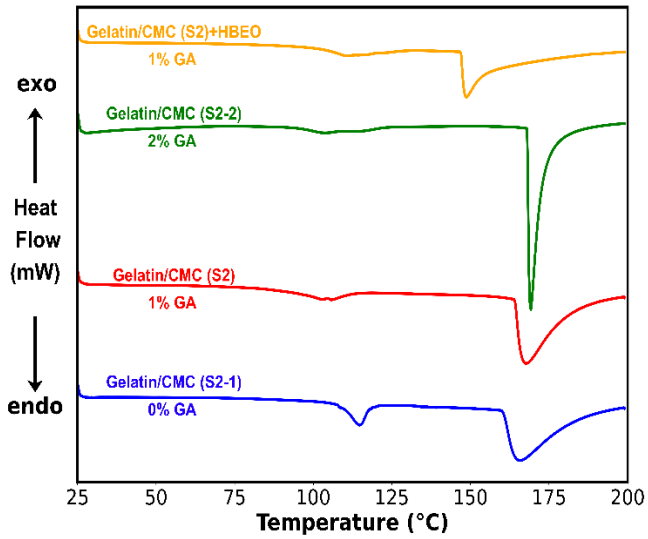

Figure 6. DSC thermogram of gelatin/CMC composite hydrogels with varying concentrations of GA.

3.2.3 Thermal properties of gelatin/CMC hydrogels

DSC thermograms of the gelatin/CMC hydrogels with varying crosslinker GA concentrations and with/without HBEONE incorporation are presented in Figure 6. The pristine gelatin/CMC hydrogel (S2-1, 0% GA) exhibited 1st endothermic transition around 110°C to 120°C, corresponding to the helix–coil transition of gelatin and bound water evaporation. The second endothermic peak appeared at 165°C, corresponding to the melting temperature (T_m) of gelatin/CMC hydrogel. With increasing GA concentration from 0% to 2%, a slight shift of the Tm toward higher values was observed, indicating the improvement in thermal stability. However, upon incorporation of HBEONE into the gelatin/CMC (S2) matrix crosslinked with 1% GA, a remarkable decrease in the T_m was detected. This reduction suggests that the embedded HBEONE droplets disrupted the polymer–polymer hydrogen bonding and partially interfered with the crosslinking network, leading to a more flexible structure and reduced thermal resistance [33].

3.2.4 Morphological observations

The cross-sectional morphology of the hydrogels was examined by scanning electron microscopy (SEM), as shown in Figure 7. The neat gelatin (S1) hydrogel exhibited a relatively smooth and less porous structure. Upon incorporating CMC into the hydrogel matrix (sample S2), the morphology became more porous, reflecting improved water absorption and interconnectivity between the polymer chains. With a further increase in CMC content (sample S3), SEM images revealed a looser and more open network structure, suggesting enhanced flexibility and swelling capacity due to reduced intermolecular interactions within the hydrogel matrix.

Moreover, the cross-sectional images showed that increasing the GA concentration from 1% to 2% produced a denser and more compact internal structure, consistent with higher crosslinking density and reduced pore volume [34]. Following the incorporation of HBEONE into the hydrogel matrix, the pore size became smaller, attributed to the distribution of HBEO-NE within the polymer network.

3.2.5 Swelling behavior of gelatin/CMC hydrogels

The swelling behavior of the Gelatin/CMC hydrogel studied over a 24 h duration was shown in Figure 8(a). Pure gelatin (S1) with 1% GA showed the lowest swelling ratio. Adding CMC at a 1:1 ratio (S3), the swelling degree was enhanced 2.5 times compared to neat gelatin (S1). This result indicates that the hydrophilic CMC showed more water absorption [20]. On the other hand, increasing crosslinker GA from 1% to 2% reduced the swelling ratios of S2 gelatin/CMC from 8 ($g \cdot g^{-1}$) to 6.5 ($g \cdot g^{-1}$), respectively. Furthermore, the swelling behavior of HBEONE-loaded hydrogels showed a moderate decrease compared to unloaded hydrogels, which can be attributed to the partial occupation of the hydrogel pores by HBEONE droplets, thereby restricting water absorption and swelling.

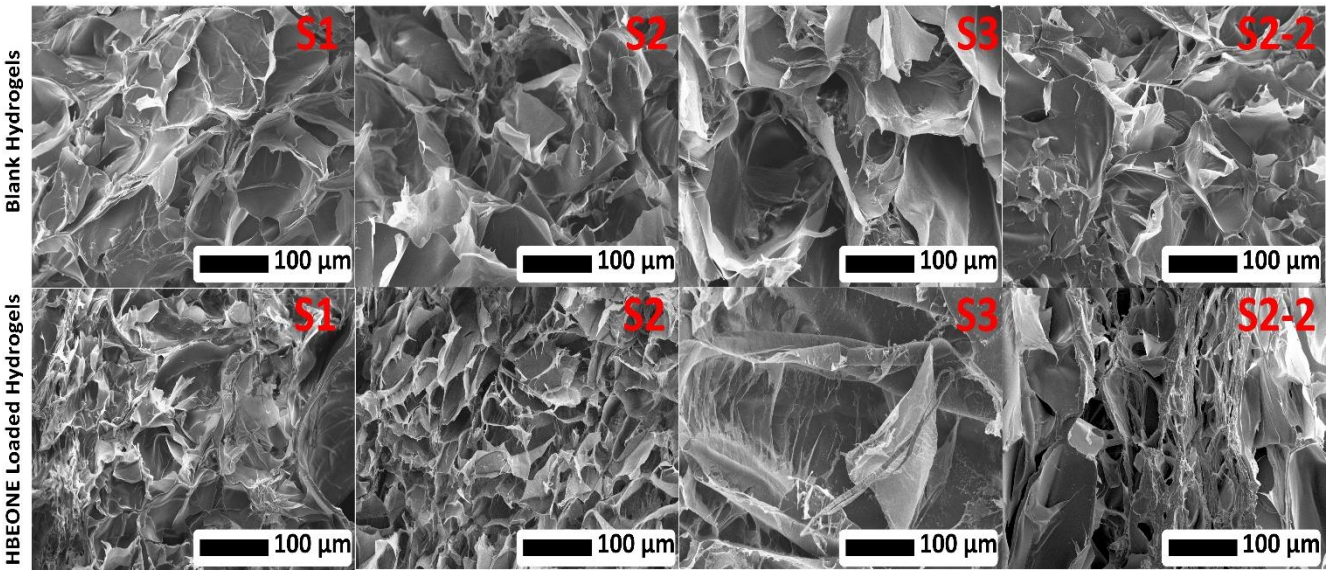

Figure 7 Cross-sectional morphology of hydrogels (S1) gelatin, (S2) gelatin/CMC(3/1) at 1% GA, (S3) gelatin/CMC(1/1) at 1% GA, (S2-2) gelatin/CMC (3/1) at 2% GA.

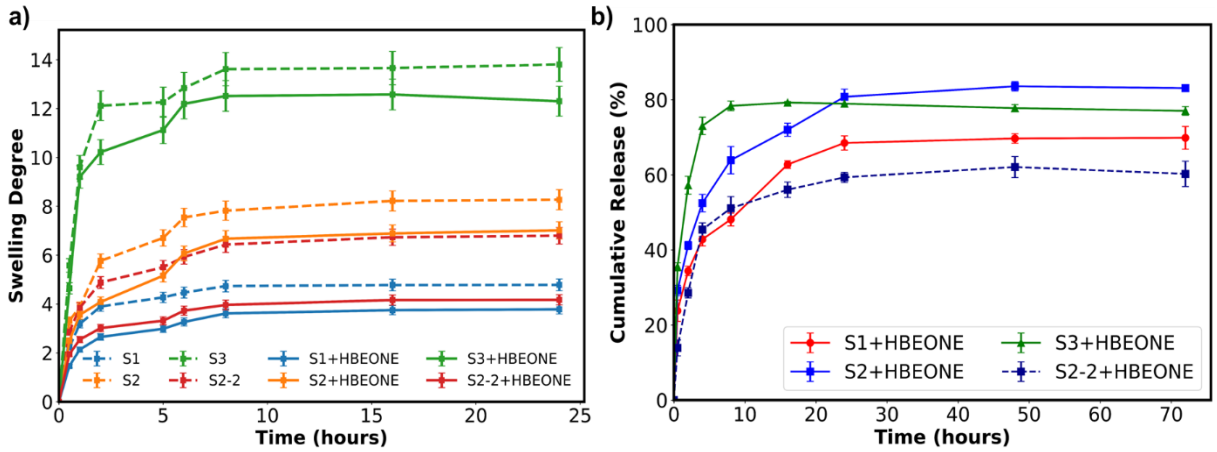

Figure 8. (a) Swelling behavior of gelatin/CMC composite hydrogels, and (b) In vitro HBEO release study of hydrogels.

3.2.6 In vitro HBEO release study from composite hydrogels

The in vitro release profiles of HBEONE-entrapped gelatin/CMC hydrogel formulations were shown in Figure 8(b). Among all hydrogels, the S3 formulation with a higher CMC amount showed the quickest release (80% release in the first 10 h). In contrast, S1, S2, and S2-2 displayed lower release of the HBEO. Since S3 contains the highest CMC content, which enhances hydrophilicity and makes it easier to uptake HBEONE and facilitates easier diffusion compared to the neat gelatin (S1). Furthermore, the hydrogel prepared with 2% crosslinker GA (S2-2) demonstrated the lowest swelling and reduced uptake of the HBEONE compared to the 1% crosslinker formulation (Table 3), thus it had a lower release of HBEO.

To understand the release mechanism of these hydrogel systems, the release profiles of the resulting hydrogels were fitted to several kinetic models, as summarized in Table 4. The correlation coefficient (R^2) values indicate that Korsmeyer–Peppas models best fit the release data, suggesting that the drug release follows diffusion-controlled and Fickian mechanisms. As a result, these findings revealed that the HBEO release from gelatin and gelatin/CMC hydrogels was primarily governed by a diffusion mechanism based on Korsmeyer–Peppas with $n < 0.45$ [23].

3.2.6 Antioxidant activity of HBEONE-loaded hydrogel

As shown in Figure 9, the HBEONE-loaded hydrogel exhibited a markedly higher radical-scavenging activity than the blank hydrogel throughout the 72 h. The antioxidant inhibition increased steadily from about 20% at 1 h to nearly 60% at 24 h, maintaining that level up to 72 h, indicating a sustained release of HBEO's phenolic constituents. In contrast, the blank hydrogel showed negligible activity (<5%), confirming that the antioxidant effect arose solely from the encapsulated HBEO.

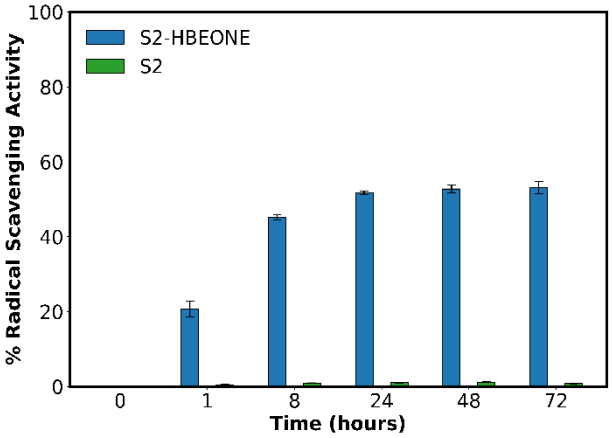

Figure 9. Comparison of antioxidant activity of HBEONE-entrapped gelatin/CMC hydrogel and the gelatin/CMC hydrogel.

Table 3. Gelatin/CMC hydrogels and their HBEONE loading capacities.

Sample	Gelatin/CMC ratio	GA [%]	HBEONE loading [%]
S1	1/0	1	58
S2	3/1	1	67.5
S3	1/1	1	72.7
S2-2	3/1	2	55.4

Table 4. Fitting parameters of different kinetic models for HBEO release from gelatin/CMC hydrogels entrapping HBEONE.

Sample	Zero-order	First-order	Higuchi	Korsmeyer–peppas		
	R^2	R^2	R^2	k_{KP}	n	R^2
S1	0.61	0.68	0.82	0.30	0.230	0.96
S2	0.60	0.72	0.81	0.37	0.222	0.95
S3	0.23	0.24	0.42	0.49	0.141	0.71
S2-2	0.45	0.52	0.67	0.23	0.284	0.84

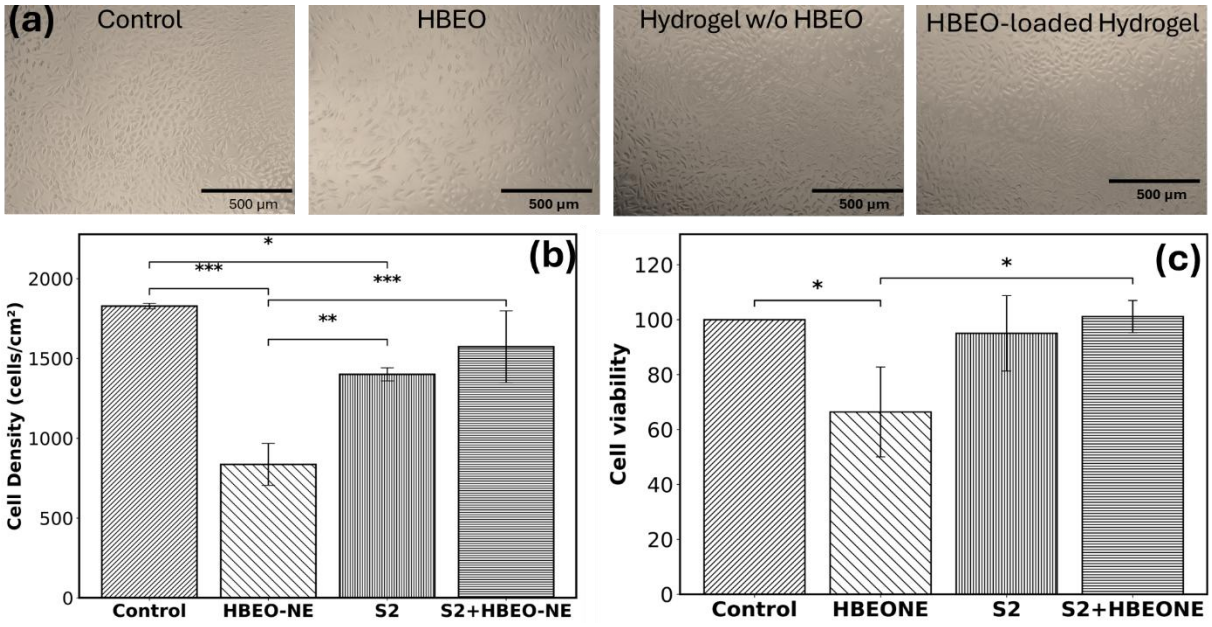

Figure 10. (a) The microscopy images, (b) % cell density, and (c) cell viability of control, HBEO, hydrogel S2, and S2+HBEONE sample. Data are presented as mean ± SD (n = 3). Statistical analysis was performed by one-way ANOVA followed by Tukey's post-hoc test, with the criterion for statistical significance as follows: * significant at $p < 0.05$, ** significant at $p < 0.01$, and *** significant at $p < 0.001$.

3.2.7 Cytotoxicity test (MTT assay)

The cytotoxicity of HBEO, gelatin/CMC hydrogel, and HBEO-NE-loaded gelatin/CMC hydrogel was assessed using the MTT assay, as shown in Figure 10. Microscopic observations revealed that the hydrogel-treated groups supported uniform cell distribution and morphology, indicating good cell attachment and proliferation comparable to the control group. In contrast, cells treated with pure HBEO exhibited a marked decrease in cell number, showing approximately 66.4% viability relative to the control. This reduction may be attributed to the burst release of HBEO, leading to temporary cytotoxic effects and possible apoptosis. Meanwhile, incorporation of HBEONE into the hydrogel matrix displayed a considerable improvement in cell viability compared to neat HBEO. These results confirm that encapsulated HBEONE within the gelatin/CMC hydrogel effectively mitigates its direct cytotoxicity while maintaining biocompatibility, providing a safer and more suitable platform for biomedical applications.

4. Conclusion

The integration of HBEO nanoemulsion into a gelatin/CMC hydrogel addressed the limitations of free HBEO by improving its solubility, stability, and controlled release. The HBEONE (1% HBEO in 0.5% PVA) achieved nanosized droplets (182±3 nm, PDI = 0.286) with a sustained 92% release. Once dispersed in the S2 gelatin/CMC network, the composite hydrogel combined high water uptake (swelling ratio ≈8 $g \cdot g^{-1}$) with substantial loading (≈67.5%), supporting prolonged HBEO availability. Functionally, the system preserved HBEO's sustained antioxidant response while reducing cytotoxicity versus free HBEO in L929 cells, indicating that nanoencapsulation and matrix-mediated diffusion effectively mitigate concentration spikes that can trigger apoptosis.

Acknowledgements

This work was supported by Graduate Scholarship Program for ASEAN or Non-ASEAN countries, Thailand.

References

[1] D. Braatz, M. Cherri, M. Tully, M. Dimde, G. Ma, E. Mohammadifar, F. Reisbeck, V. Ahmadi, M. Schirner, and R. Haag, "Chemical approaches to synthetic drug delivery systems for systemic applications," *Angewandte Chemie International Editio*n, vol. no. 49, p. e202203942, 2022.

[2] R. Langer, "Drug delivery and targeting," *Nature*, vol. 30. no. 392, pp. 5–10, 1998.

[3] D. P. de Sousa, R. O. S. Damasceno, R. Amorati, H. A. Elshabrawy, R. D. de Castro, D. P. Bezerra, V. R. V. Nunes, R.C. Gomes, and T. C. Lima, "Essential oils: Chemistry and pharmacological activities," *Biomolecules*, vol. 13, no. 7, p. 1144, 2023.

[4] A. Bhatnagar, and R. Pimoli, "Chemical composition of the essential oil of Ocimum sanctum L. growing in Garhwal region of Uttarakhand, India," *International Journal of Herbal Medicine*, vol. 13, no. 2, pp. 43–46, 2025.

[5] P. Singh, B. B. Basak, V. J. Patel, R. Sarkar, K. C. Patel, G. N. Motaka, "Integration of biochar with chemical fertilizers improves the economic yield, quality of holy basil (Ocimum sanctum L.) and soil health," *Journal of Soil Science and Plant Nutrition*, vol. 24, pp. 6404–6417, 2024.

[6] M. W. Imam, and S. Luqman, "Unveiling the mechanism of essential oil action against skin pathogens: from ancient wisdom to modern science," *Archives of Microbiology*, vol. 206, no. 8, p. 347, 2024.

[7] R. J. Wilson, Y. Li, G. Yang, and C.-X. Zhao, "Nanoemulsions for drug delivery," Particuology, vol. 64, pp. 85–97, 2022.

[8] Z. Yang, Q. He, B. B. Ismail, Y. Hu, and M. Guo, Ultrasonication induced nano-emulsification of thyme essential oil: Optimization and antibacterial mechanism against Escherichia coli," *Food Control*, vol. 133, p. 108609, 2022.

[9] Y. Shi, M. Zhang, K. Chen, and M. Wang, "Nano-emulsion prepared by high pressure homogenization method as a good carrier for Sichuan pepper essential oil: Preparation, stability, and bioactivity, *LWT*, vol. 154, p. 112779, 2022.

[10] Z. Xing, Y. Xu, X. Feng, C. Gao, D. Wu, W. Cheng, L. Meng, Z. Wang, T. Xu, and X. Tang, "Fabrication of cinnamon essential oil nanoemulsions with high antibacterial activities via microfluidization," *Food Chemistry*, vol. 456, p. 139969, 2024.

[11] L. Zhou, W. Zhang, J. Wang, R. Zhang, and J. Zhang, "Comparison of oil-in-water emulsions prepared by ultrasound, high-pressure homogenization and high-speed homogenization," *Ultrasonics Sonochemistry*, vol. 82, p. 105885, 2022.

[12] R. Song, Y. Lin, and Z. Li, "Ultrasonic-assisted preparation of eucalyptus oil nanoemulsion: Process optimization, in vitro digestive stability, and anti-Escherichia coli activity," *Ultrasonics Sonochemistry*, vol. 82, p. 105904, 2022.

[13] C. Laosinwattana, N. Somala, J. Dimak, M. Teerarak, and N. Chotsaeng, "Ultrasonic emulsification of Cananga odorata nanoemulsion formulation for enhancement of herbicidal potential," *Scientific Reports*, vol. 15, p. 3263, 2025.

[14] P. Pongsumpun, S. Iwamoto, and U. Siripatrawan, "Response surface methodology for optimization of cinnamon essential oil nanoemulsion with improved stability and antifungal activity, "*Ultrasonics Sonochemistry*, vol. 60, p. 104604, 2020.

[15] Y. Weerapol, S. Manmuan, N. Chaothanaphat, S. Okonogi, C. Limmatvapirat, S. Limmatvapirat, and S. Tubtimsri, "Impact of fixed oil on ostwald ripening of anti-oral cancer nanoemulsions loaded with amomum kravanh essential oil," *Pharmaceutics*, vol. 14, p. 938, 2022.

[16] N. M. Deghiedy, N. M. Elkenawy, and H. A. Abd El-Rehim, "Gamma radiation-assisted fabrication of bioactive-coated thyme nanoemulsion: A novel approach to improve stability, antimicrobial and antibiofilm efficacy," *Journal of Food Engineering*, vol. 304, p. 110600, 2021.

[17] V. S. Ghorpade, R. J. Dias, K. K. Mali, and S. I. Mulla, "Citric acid crosslinked carboxymethylcellulose-polyvinyl alcohol hydrogel films for extended release of water soluble basic drugs," *Journal of Drug Delivery Science and Technology*, vol. 52, p. 421–430, 2019.

[18] M. S. Manga, L. Higgins, A. A. Kumar, B. T. Lobel, D. W. York, and O. J. Cayre, "Exploring effects of polymeric stabiliser molecular weight and concentration on emulsion production via stirred cell membrane emulsification," *Polymer Chemistry*, vol. 14, pp. 5049–5059, 2023.

[19] E. J. Delgado-Pujol, G. Martínez, D. Casado-Jurado, J. Vázquez, J. León-Barberena, D. Rodríguez-Lucena, Y. Torres, A. Alcudia, and B. Begines, "Hydrogels and nanogels: Pioneering the future of advanced drug delivery systems," *Pharmaceutics*, vol. 17, p. 215, 2025.

[20] R. Andreazza, A. Morales, S. Pieniz, and J. Labidi, "Gelatin-based hydrogels: Potential biomaterials for remediation," *Polymers (Basel)*, vol. 15, p. 1026, 2023.

[21] W. Zhang, Y. Liu, Y. Xuan, and S. Zhang, "Synthesis and applications of carboxymethyl cellulose hydrogels," *Gels*, vol. 8, p. 529, 2022.

[22] N. Kreua-Ongarjnukool, S. T. Niyomthai, K. Sarodom, T. Lothong, and N. Soomherun, "Hybrid gelatin/carboxymethyl cellulose hydrogel loaded copper(II) ion for medical applications, *Materials Science Forum*, vol. 1009, pp. 3–8. 2020.

[23] F. Sahar, A. Riaz, N. S. Malik, N. Gohar, A. Rasheed, U. R. Tulain, A. Erum, K. Barkat, S. F. Badshah, and S. I. Shah, "Design, characterization and evaluation of gelatin/carboxymethyl cellulose hydrogels for effective delivery of ciprofloxacin, *Polymer Bulletin*, vol. 80, no. 11, pp. 12271–12299, 2022.

[24] B. He, Y. Wang, Z. Jiang, S. Liu, and J. Zhu, "Physical properties and antibacterial activity of the composited films based on carboxymethyl cellulose and gelatin functionalized with ε-polylysine," *International Journal of Biological Macromolecules*, vol. 191, pp. 1126–1136, 2021.

[25] A. Hivechi, M. T. Joghataei, S. H. Bahrami, P. B. Milan, M. Amoupour, N. Latifi, S. M. A. Haramshahi, S. Naderi Gharahgheshlagh, and S. Nezari, "Oxidized carboxymethyl cellulose/gelatin in situ gelling hydrogel for accelerated diabetic wound healing: Synthesis, characterization, and in vivo investigations," *International Journal of Biological Macromolecules*, vol. 242, p. 125127, 2023.

[26] A. Bigi, G. Cojazzi, S. Panzavolta, K. Rubini, and N. Roveri, "Mechanical and thermal properties of gelatin films at different degrees of glutaraldehyde crosslinking," *Biomaterials*, vol. 22, pp. 763–768, 2001.

[27] R. Parveen, S. Baboota, J. Ali, A. Ahuja, and S. Ahmad, "Stability studies of silymarin nanoemulsion containing Tween 80 as a surfactant," *Journal of Pharmacy and Bioallied Sciences*, vol. 7, p. 321, 2015.

[28] K. Flekka, V. D. Dimaki, E. Mourelatou, K. Avgoustakis, F. N. Lamari, and S. Hatziantoniou, "Stability and retention of nanoemulsion formulations incorporating lavender essential oil, *Cosmetics*, vol. 11, no. 3, p. 65, 2024.

[29] A. Kaolaor, K. Kiti, P. Pankongadisak, and O. Suwantong, "Camellia Oleifera oil-loaded chitosan nanoparticles embedded in hydrogels as cosmeceutical products with improved biological properties and sustained drug release," *International Journal of Biological Macromolecules*, vol. 275, p. 133560, 2024.

[30] T. M. Tran Vo, P. Potiyaraj, P. del Val, and T. Kobayashi, "Ultrasound-triggered amoxicillin release from chitosan/ethylene glycol diglycidyl ether/amoxicillin hydrogels having a covalently bonded network," *ACS Omega*, vol. 9, p. 585, 2023.

[31] F.N. Sorasitthiyanukarn, P. Rojsitthisak, and P. Rojsitthisak, "Kinetic study of chitosan-alginate biopolymeric nanoparticles for the controlled release of curcumin diethyl disuccinate," *Journal of Metals, Materials and Minerals*, vol. 27, no. 2, pp. 17-22, 2017.

[32] T. M. Tran Vo, P. Sanghong, A. Pongwisuthiruchte, C. Aonbangkhen, X. Chen, and P. Potiyaraj, "Self-oxygenating, autonomous self-healing dual-physical crosslinked PVA/chitosan/hydrolysed collagen hydrogels for advanced wound management," *Journal of Materials Chemistry B*, vol. 13, pp. 11020–11031, 2025.

[33] Y. Qin, W. Li, D. Liu, M. Yuan, and L. Li, "Development of active packaging film made from poly (lactic acid) incorporated essential oil," *Progress in Organic Coatings* , vol. 103. pp. 76–82, 2017.

[34] G. Mugnaini, R. Gelli, L. Mori, and M. Bonini, "How to cross-link gelatin: the effect of glutaraldehyde and glyceraldehyde on the hydrogel properties," *ACS Applied Polymer Materials*, vol. 5, pp. 9192–9202, 2023.